High Accuracy Calculation of the
Magnetic Vector Potential On Surfaces

Malcolm M. Bibby* and Andrew F. Peterson**
*Gullwings, Weston, MA 02493 e-mail: mbibby@gullwings.com
**Georgia Institute of Technology, Atlanta, GA; e-mail: peterson@ee.gatech.edu

Abstract. The calculation of integrals containing the free-space Green's function in electromagnetic problems is difficult to perform with great accuracy. Three approaches to the calculation are investigated. The inadequacy of the singularity-subtraction method is demonstrated. The Duffy transform is shown to provide good results when the test-point is on the surface being investigated. A Maclaurin series expansion with integration prior to summation is shown to be efficient and reliable both on and off the surface under study. Solutions, in both Cartesian and cylindrical coordinate systems, that allow the calculations to be performed to a pre-defined level of accuracy are presented.

Introduction.

The magnetic vector potential, or MVP, is an important quantity that appears in many electromagnetic problems that involve evaluation of electric and/or magnetic fields. For example, it is a component in the definition of the electric field integral equation, EFIE [1, p17]. In this context it may exist in its basic form or it may be subject to differentiation. Its use is at its most basic when used in the solution of Hallen's integral equation for a cylindrical dipole. When used for solving Pocklington's integro-differential equation for the same dipole the second differential of the MVP must be considered. Derivatives of the MVP are also derivatives of the Green's function contained within the definition of the MVP. Because the three-dimensional Green's function contains a singularity, it is preferable to keep the order of differentiation to a minimum, preferably zero. When it cannot be kept to zero, then one of two actions are generally undertaken. Either the derivatives must be transferred to the basis/testing function used in the solution of the particular EFIE under investigation or one of the special formulations that have been developed to accommodate the differentiation [2] [3] must be considered. Even when one examines the evaluation of just the non-differentiated form of the MVP one has certain numerical difficulties to face. These difficulties are addressed in this report. Accurate evaluation of the MVP is gaining importance as the use of higher and higher order basis functions is considered. Also, as we shall see, evaluation of the MVP when the test-point is located a short distance from the test surface is a requirement that, while of interest in many applications, is handled poorly by current techniques.

As the title of this paper suggests, the over-riding issue here is one of solution accuracy. When calculating entries in a matrix, Z, and then solving the corresponding matrix equation, $ZI = V$, Miller [4] has shown that the solution error, $\|dI\|/\|I\|$, is comparable to the product of the error in the terms in the matrix and the condition number of the matrix. For example, if the error of the matrix terms, $\|dZ\|/\|Z\|$, is 10^{-6} and the condition number is 10^{4}, the error of the solution may be no better than 10^{-2} - if nothing else introduces further errors. The resulting accuracy is at the lower limit of usefulness. It can be improved by either reducing the condition number of the

matrix or by reducing the error in the calculation of the matrix entries. This work is about the latter.

After setting out some basic definitions, this report will investigate the difficulties associated with the most widely used approach to the evaluation of the MVP. The second section will examine the use of the Duffy [5] transform which was originally conceived to address issues arising in the evaluation of integrals such as found in the MVP. The third section will show how the MVP can be dealt with in a manner that is not only rigorous but also efficient. This will be followed by a discussion of testing, concluding with a statement of key findings.

Definitions.

The three-dimensional MVP is defined as:

$$I_3 = \iiint \overline{J}(\overline{r}') \frac{e^{-jk|\overline{r}-\overline{r}'|}}{4\pi|\overline{r}-\overline{r}'|} dv' \qquad (1)$$

When examining currents on surfaces, this definition reduces to:

$$I_2 = \iint \overline{J}(\overline{r}') \frac{e^{-jk|\overline{r}-\overline{r}'|}}{4\pi|\overline{r}-\overline{r}'|} dv' \qquad (2)$$

In the above, $\overline{r}$ denotes the position vector to the test/observation point, and $\overline{r}'$ is the position vector to the surface under study. The scalar component(s), I_s, of the surface current will be represented by polynomials, in u, in the form: $I_s = \sum_{i=0}^{p} a_i u^i$.

Machine precision will be referred to often in this study. By machine precision we will be referring to machine epsilon, ε, which is the gap between 1 and the next larger floating point number [6, p14]. $\varepsilon = 2^{-(p-1)}$ where p is the precision of the machine in bits. Machine precision is:

$$\log_{10}(\varepsilon) = -(p-1)\log_{10}(2) \qquad (3)$$

Results for Compaq Fortran on an Alpha processor are shown in Table I.

Relative error, Rel. error, is defined as:

$$\text{Rel. error} = \frac{|f_{approx} - f_{ref}|}{|f_{ref}|}. \qquad (4)$$

f_{ref} will be defined each time that relative error is discussed. When evaluating integrals one frequently compares the result, f_n, obtained in the most recent evaluation, to the result, f_{n-1} obtained in the prior evaluation. This is more accurately defined as convergence rate and:

$$\text{Convergence Rate} = \frac{|f_n - f_{n-1}|}{|f_n|} \qquad (5)$$

Singularity Subtraction.

The free-space Green's function is defined as $G(R) = e^{-jkR}/R$ where R is the distance between the source and the observation or test point. The mathematical definition of R is specific to the coordinate system in use and will be elaborated on later. For this section of the report we define $R = \sqrt{u^2 + \delta^2}$ where u is an independent variable and δ will assume various fixed values. $G(R)$ is split into two parts $G(R) = G_r(R) + G_s(R)$, where $G_r(R)$ is the non-singular part and $G_s(R)$ is the singular part [7]. Specifically, we have:

$$G_r(R) = e^{-jkR}/R - 1/R_0 \qquad (6a)$$

$$G_s(R) = 1/R_0 \qquad (6b)$$

$G_s(R)$ is developed from a Taylor series expansion of $G(R)$ and when possible it is evaluated analytically [8]. An example of a solution in the Cartesian coordinate system is given in [1, p420]. In the event an analytical solution is not available, a recent discussion

Figure 1. Plots of the real and imaginary parts of G(R) as a function of u.
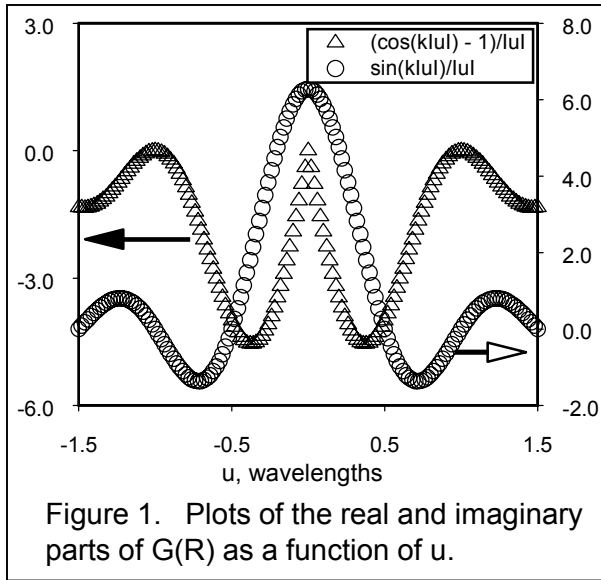
of numerical methods is available in [9]. The focus in the following is on $G_r(R)$.

For purposes of this immediate analysis we express $G_r(R)$ in terms of its real and imaginary components:

$$G_r(R) = (\cos(kR) - 1)/R - j\sin(kR)/R \qquad (7)$$

These two components, when $R = |u|$ (i.e. $\delta = 0$) are plotted in Figure 1. Both components are finite throughout the range. However, the real component is obviously not 'smooth' at $u = 0.0$.

The results for integrating the real component of $G_r(R)$ with Gauss-Legendre quadrature are plotted in Figure 2a, where d is the same as δ in the text. The reference values were calculated using the series expansion method described later. It is observed that the integration convergence becomes worse as $\delta \to 0$, a finding which is somewhat unexpected, counter-intuitive and disconcerting. A similar observation is implied in Figure 2 in [10].

When evaluating integrals numerically, particularly close to the source, it is important to remember that integration rules generally exhibit an error that is proportional to the derivatives of the function being integrated.

Figure 2a. The effect of d on the relative error in the integration of the real part of the Green's function.
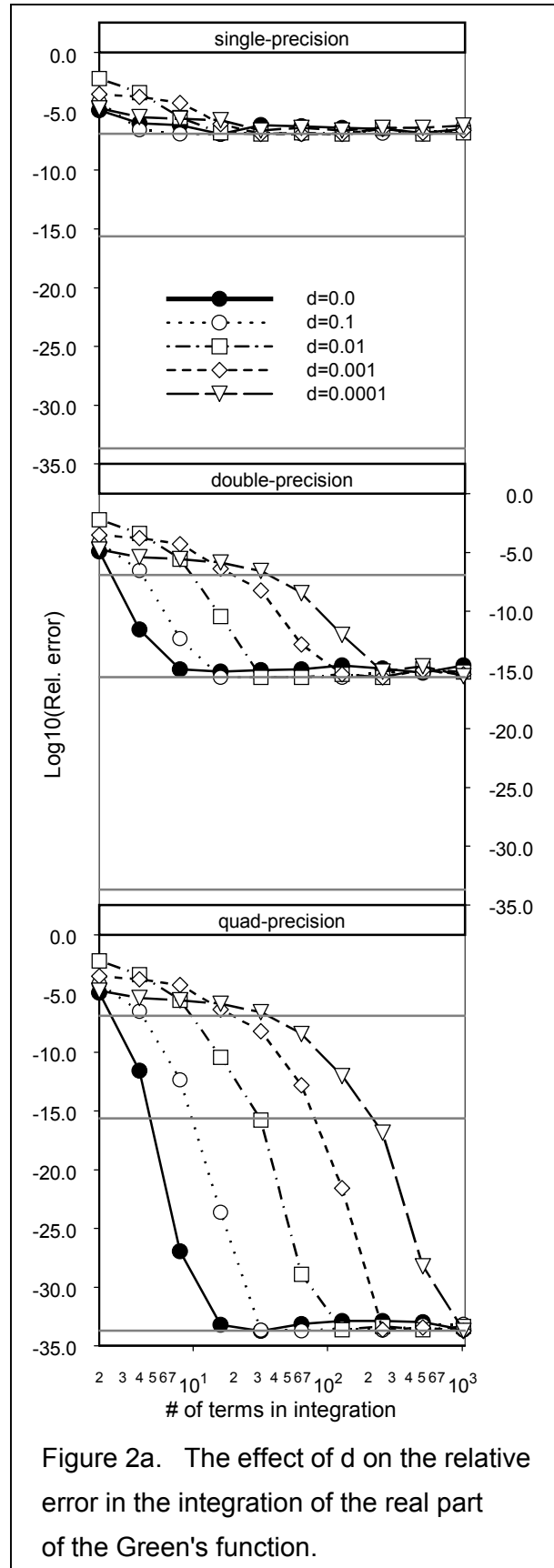
In the case of: $f = (\cos(kR) - 1)/R$ (8a)

then $\dfrac{df}{du} \approx \dfrac{-k^2 u}{2R}$ (8b)

and $\dfrac{d^2 f}{du^2} \approx -\dfrac{k^3 u^2}{3R^2} - \dfrac{k^2 \delta^2}{2R^3}$ (8c)
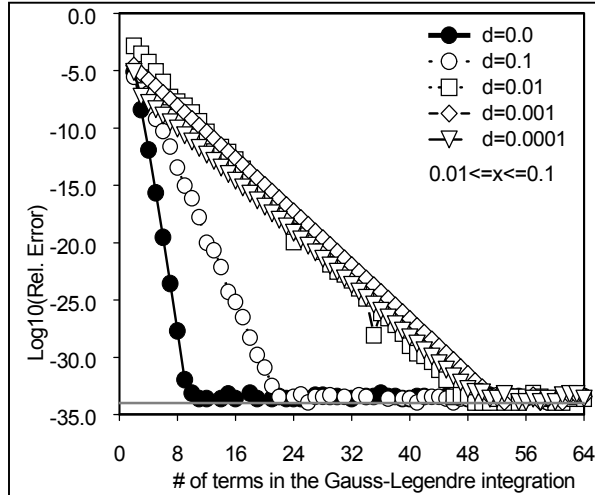
Figure 2b. Effect of n on the integration of (cos(k|R|) - 1)/R when x is not at the origin.

From this last equation we see that as:

$$u \to 0, \; \frac{d^2 f}{du^2} \to -\frac{k^2}{2\delta} \qquad (8d)$$

which provides an explanation for the behavior of the curves in Figure 2a. To illustrate that it is, in fact, the presence of the discontinuity at $u = 0$ that creates the problems, the lower limit of integration was moved from $u = 0$ to $u = 0.01$. The results of this change are shown in Figure 2b and clearly demonstrate that the problem has been significantly mitigated.

For the special case of $\delta = 0$, we find that although there is a jump in the values of $\dfrac{df}{du}, \dfrac{d^2 f}{du^2}$ and higher derivatives when u moves from 0_- to 0_+ they are finite in that region nevertheless, and so the integration rules hold for this special case.

For double/triple integrals δ is introduced into the inner integral by the outer integral defining the MVP and thus δ may become arbitrarily

---

$$I_{cart} = \int_0^{x_1}\int_0^{y_1} \frac{e^{-jkr}}{r} dxdy = \int_0^{x_1} dx \int_0^{Kx} \frac{e^{-jkr}}{r} dy + \int_0^{y_1} dy \int_0^{y/K} \frac{e^{-jkr}}{r} dx \text{ where } r = \sqrt{x^2 + y^2 + z_0^2} \text{ and } K = y_1/x_1$$

Substituting $y = uKx$ and $x = vy/K$ in the inner integrals, we arrive at:

$$I_{cart} = \int_0^{x_1} dx \int_0^1 \frac{e^{-jkr} du}{\sqrt{u^2 + (1/K)^2 + (z_0/Kx)^2}} + \int_0^{y_1} dy \int_0^1 \frac{e^{-jkr} dv}{\sqrt{v^2 + K^2 + (z_0 K/y)^2}} \qquad (9)$$

$$I_{cyl} = \int_0^{\pi/2}\int_0^{z_1} z^p \frac{e^{-jkr}}{r} d\theta\, dz = \int_0^{\pi/2} d\theta \int_0^{\theta/K} z^p \frac{e^{-jkr}}{r} dz + \int_0^{z_1} z^p dz \int_0^{Kz} \frac{e^{-jkr}}{r} d\theta$$

where $r = \sqrt{z^2 + \Delta\rho_0^2 + 4a(a + \Delta\rho_0)\sin^2\theta}$, K$=\dfrac{\pi}{2z_1}$

Substituting $z = u\theta/K$ and $\theta = vKz$ in the inner integrals we obtain:

$$I_{cyl} = \int_0^{\pi/2} d\theta \int_0^1 \frac{(u\theta/K)^p e^{-jkr} du}{\sqrt{u^2 + 4a(a + \Delta\rho_0)(K\sin\theta/\theta)^2 + (K\Delta\rho_0/\theta)^2}} +$$

$$\int_0^{z_1} z^p dz \int_0^1 \frac{e^{-jkr} dv}{\sqrt{(1/K)^2 + 4a(a + \Delta\rho_0)(\sin(vKz)/Kz)^2 + (\Delta\rho_0/Kz)^2}} \qquad (10)$$

Equation Set 1. The MVP equation, expressed in two different coordinate systems, transformed, by the Duffy method, to remove the singularity at the origin.

small, but non-zero, leading to these problems. Consequently, when evaluating the real part of $G_r(R)$, it would appear that all quadrature rules, when applied directly, are doomed to fail as even the simple trapezoid rule requires that the second derivative of the integrand be well behaved. With this conclusion it is advisable to seek alternative methods.

Singularity Removal by Transformation.

In 1982, Duffy [5] proposed a method that, through a change of variable, causes the removal of the singularity in the integrand of two and three dimensional integrals. His method is presented here first with a constant current, for simplicity, in the Cartesian coordinate system. Currents of polynomial form u^p, are included with the discussion of the cylindrical coordinate system.

The formalism for each of the two coordinate systems is shown in Equation Set 1. It allows for the test/observer point to be offset from the surface – by amount z_0 in the Cartesian system and $\Delta\rho_0$ in the cylindrical system.

When the offset is zero, the formulae in the Cartesian system clearly show that the singularity has been removed. Furthermore, in this case, the denominator in the integrand is not dependant on the variable associated with the outer loop other than through the value of K, which is fixed. Consequently, the derivatives of the integrand are all well behaved and one can expect that quadrature integration will work well, and indeed it does.

Precision	ε	Outer Integral	Inner Integral
Single	1.2E-07	7	7
Double	2.3D-16	7	13
Quad	2.0D-34	13	37

Table I. The number of terms required in one of the double integrals for a square domain using the Duffy transform.

For example, using Gauss-Legendre for both the inner and outer integrals, the numbers of terms necessary for computing the double integral, to a precision of 2ε, on a flat surface are shown in Table 1. The dimensions of the cell were $0.0 \leq x \leq 0.1,\ 0.0 \leq y \leq 0.1$. Because of symmetry in this example, the numbers of terms, required in the two double integrals, are the same. All the integrals terminate when the convergence rate falls below the precision level, 2ε.

When examining a cylindrical case we look at a cell width of 0.1 wavelengths on a cylinder of radius 0.007 wavelengths. In addition, polynomial representations of the current, to the degree p, are incorporated. Again, the examination takes place on the surface, so that $\Delta\rho_0 = 0$. For this case we track the number of terms in the outer(out) and inner(in) integrals for the two transformed double integrals. We identify these as u-out, u-in, v-out and v-in. The results, calculated in double precision to a precision level of 2ε, are shown in Table II. They indicate no dependence between the degree, p, and the number of terms.

p	u-out	u-in	v-out	v-in	Total
0	11	36	8	10	476
1	9	38	9	10	432
2	10	36	10	9	450
3	13	34	9	10	532
4	12	29	10	9	438
5	11	29	10	9	409

Table II. The number of terms required in each of the integrals for the cylindrical surface using the Duffy transform.

The good performance of the Duffy transform when the offset is zero does not follow through when the offset is some finite value. This is revealed when the data of Table III is examined. This table shows the total number of iterations needed by the integrals as a function of the value of the offset, $\Delta\rho_0$. The dimensions on a cylindrical surface are the same as used in Table II. A value of $p = 0$ was used.

Offset	Duffy	G-L
0.0	476	N/A
0.0001	12280	4356
0.001	4504	1860
0.01	1370	952
0.1	311	143

Table III. The effect of the offset value on the number of integration terms for the cylindrical surface using the Duffy transform and Gauss-Legendre applied directly to the double integral.

For comparative purposes Table III also shows the results when the MVP is integrated directly. This is possible when the offset is finite. We conclude that for test/observation points off the surface, the Duffy transform is unacceptably inefficient. Nevertheless, when the test/observation point is on the surface the transform offers a method that provides rigorous convergence in the integrals associated with the MVP.

A Series Expansion for $G(R)$.

The Maclaurin expansion for the real and imaginary components of the Green's function are:

$$\cos(kR)/R = 1/R - k^2 R/2! + k^4 R^3/4!...(11a)$$

$$\sin(kR)/R = k - k^3 R^2/3! + k^5 R^4/5!... \quad (11b)$$

The method proposed integrates the expansions in (11a) and (11b), term by term, until the ratio of the last term evaluated to the largest term evaluated is less than machine-precision.   In this way it is possible to develop analytical terms for the inner integral. The terms for the expansion in (11a) are shown in the series (12a)–(12d) and the terms for the expansion of (11b) are shown in (13a)–(13d). Each of these integrals is exact for a given value of δ .   The formulae are shown with a lower limit of $u = 0.0$, but this is done for convenience only.

The Green's function is rarely evaluated on a stand-alone basis; rather it is evaluated in conjunctions with a representation of the current on the surface being studied.   We will adopt the polynomial summation defined earlier.   The integrals of interest are:

$$G_{\mathrm{Re}} = \int_{u_1}^{u_2} u^p \frac{\cos(kR)}{R} du \qquad (16a)$$

$$G_{\mathrm{Im}} = \int_{u_1}^{u_2} u^p \frac{\sin(kR)}{R} du \qquad (16b)$$

The case of $p = 0$ has already been presented in equations (12) and (13).   The case for $p = 1$ is shown in equation (14) and for $p \geq 2$ the relevant equation is (15).   This last equation is applicable to the computations of both G_{Re} and G_{Im} .   Thus, once the terms for $p = 0$ and $p = 1$ have been evaluated, the evaluations for higher values of p are straightforward.

The Series Expansion, Integration and Summation, SEIS, process described above was tested in several ways.   The first test revisits the calculations performed for use in Figure 2a.   We examine the effect of varying δ on the number of terms required to achieve convergence in the summations of the series. The results of such calculations on G_{Re} for $p = 0$, shown in Figure 3, demonstrate that the value of δ has little impact in this context and thus we conclude that a major goal of the present work has been achieved.

The second series of tests performed involved the inclusion of basis functions as discussed earlier. Shown below, in Equation Set III, are analytical expressions for some inner integrals. Using these expressions, the accuracy of the present method can be examined for the inner integral when p is odd. As a practical note, the calculation of these inner integrals (17) to high accuracy required the use of extremely high precision software. That used here was developed by Bailey [11].

$$\int_0^b \frac{du}{R} = \log(b + \sqrt{b^2 + \delta^2}) - \log(|\delta|) \tag{12a}$$

$$\int_0^b R\,du = \frac{1}{2}\left[bR_b + \delta^2 \int_0^b \frac{du}{R}\right] \quad \text{where } R_b = \sqrt{b^2 + \delta^2} \tag{12b}$$

$$\int_0^b R^3\,du = \frac{1}{4}\left[bR_b^3 + 3\delta^2 \int_0^b R\,du\right] \tag{12c}$$

$$\vdots$$

$$\int_0^b R^{2m-1}\,du = \frac{1}{2m}\left[bR_b^{2m-1} + (2m-1)\delta^2 \int_0^b R^{2m-3}\,du\right] \quad \text{where } m \geq 1 \tag{12d}$$

$$\int_0^b du = b \tag{13a}$$

$$\int_0^b R^2\,du = \int_0^b (u^2 + \delta^2)\,du = \frac{b^3}{3} + \delta^2 b \tag{13b}$$

$$\int_0^b R^4\,du = \int_0^b (u^2 + \delta^2)^2\,du = \frac{b^5}{5} + 2\delta^2 \frac{b^3}{3} + b \tag{13c}$$

$$\vdots$$

$$\int_0^b R^{2n}\,du = \int_0^b (u^2 + \delta^2)^n\,du = \frac{b^{2n+1}}{2n+1} + \frac{n\delta^2 b^{2n-1}}{2(2n-1)} \dotsb + \delta^{2n}b \tag{13d}$$

When $p = 1$

$$\int_{u_1}^{u_2} uR^{m-1}\,du = \frac{R^{m+1}}{m+1}\bigg|_{u=u_1}^{u=u_2} \quad \text{where } 0 \leq m \tag{14}$$

When $p \geq 2$, a recurrence formula can be derived which takes the form:

$$\int_{u_1}^{u_2} u^p R^m\,du = \frac{1}{p+m+1}\left[u^{p-1}R^{m+2}\bigg|_{u=u_1}^{u=u_2} - (p-1)\delta^2 \int_{u_1}^{u_2} u^{p-2}R^m\,du\right] \quad \text{where } -1 \leq m \tag{15}$$

Equation Set II. The basic equations for the term-by-term integration of a Maclaurin series expansion of the Green's function and its product with a polynomial.

The results for G_{Re} appear in Figure 4. Results for G_{Im} and G_{Re} are not visually distinguishable and hence only the results for G_{Re} are shown. The plots clearly show that, at most, 5, 8, or 14 terms, for single, double or quad precision respectively, are needed in the series expansion for this integration range. The plots also clearly show that the relative error is not dependant on p, the exponent in the basis function used to represent the current. The results presented in Figure 5, for the even values of p, are referenced with respect to their own machine precision limited values. Their behavior is similar to the results for odd values of p, which are referenced to analytical values.

single-precision

0.0
-5.0
-10.0
-15.0
-20.0
-25.0
-30.0
-35.0

d=0.1
d=0.01
d=0.001
d=0.0001

double-precision

0.0
-5.0
-10.0
-15.0
-20.0
-25.0
-30.0
-35.0

quad-precision

0.0
-5.0
-10.0
-15.0
-20.0
-25.0
-30.0
-35.0

$0.0 <= x <= 0.1$

0 2 4 6 8 10 12 14 16
# of terms in series expansion
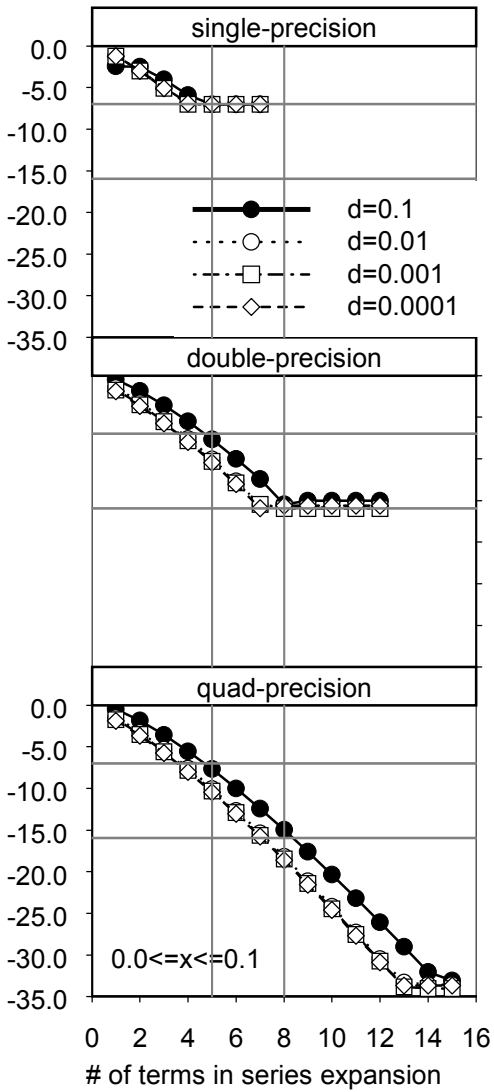
Figure 3. Convergence curves for the real component of the Green's function for different values of d.

single-precision

0.0
-5.0
-10.0
-15.0
-20.0
-25.0
-30.0
-35.0

p=1
p=3
p=5
p=7
p=9

double-precision

Log10(Rel. Error)

0.0
-5.0
-10.0
-15.0
-20.0
-25.0
-30.0
-35.0

$0.0 <= x <= 0.1;\ d=0.0$

quad-precision

0.0
-5.0
-10.0
-15.0
-20.0
-25.0
-30.0
-35.0

0 2 4 6 8 10 12 14 16
# of terms in series expansion
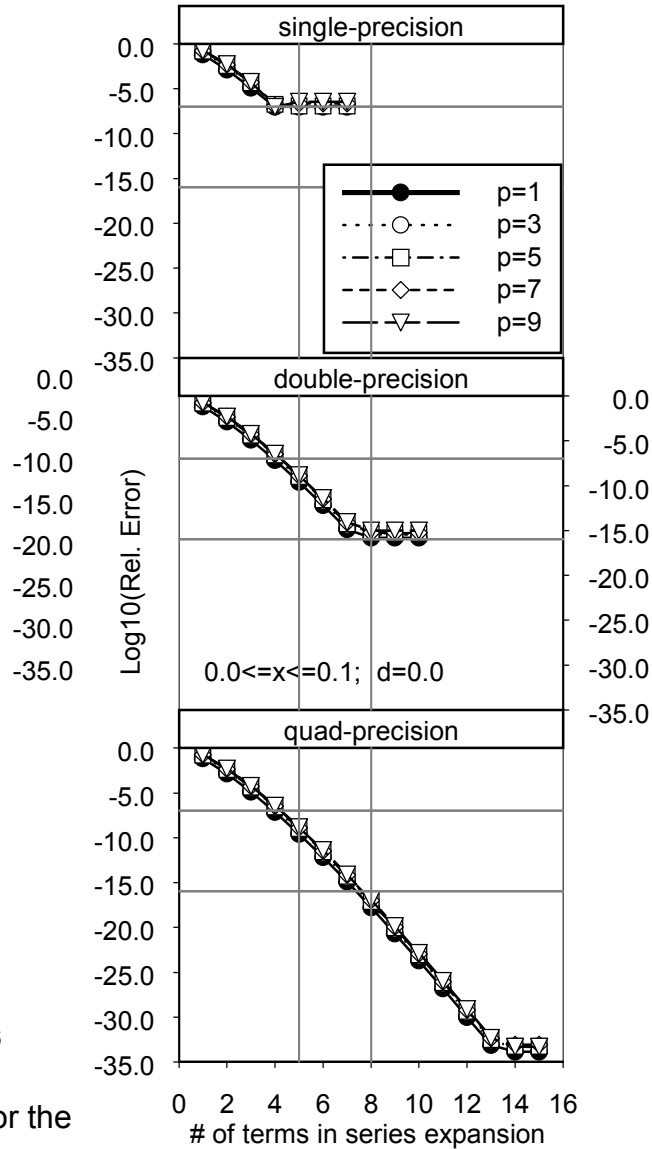
Fig4. Convergence curves for the integrals with odd powers of p.

single-precision

0.0
-5.0
-10.0
-15.0
-20.0
-25.0
-30.0
-35.0

p=2
p=4
p=6
p=8

double-precision

Log10(Rel. Error)

0.0
-5.0
-10.0
-15.0
-20.0
-25.0
-30.0
-35.0

quad-precision

0.0
-5.0
-10.0
-15.0
-20.0
-25.0
-30.0
-35.0

$0.0 <= x <= 0.1;\ d=0.0$

0 2 4 6 8 10 12 14 16
# of terms in the series expansion
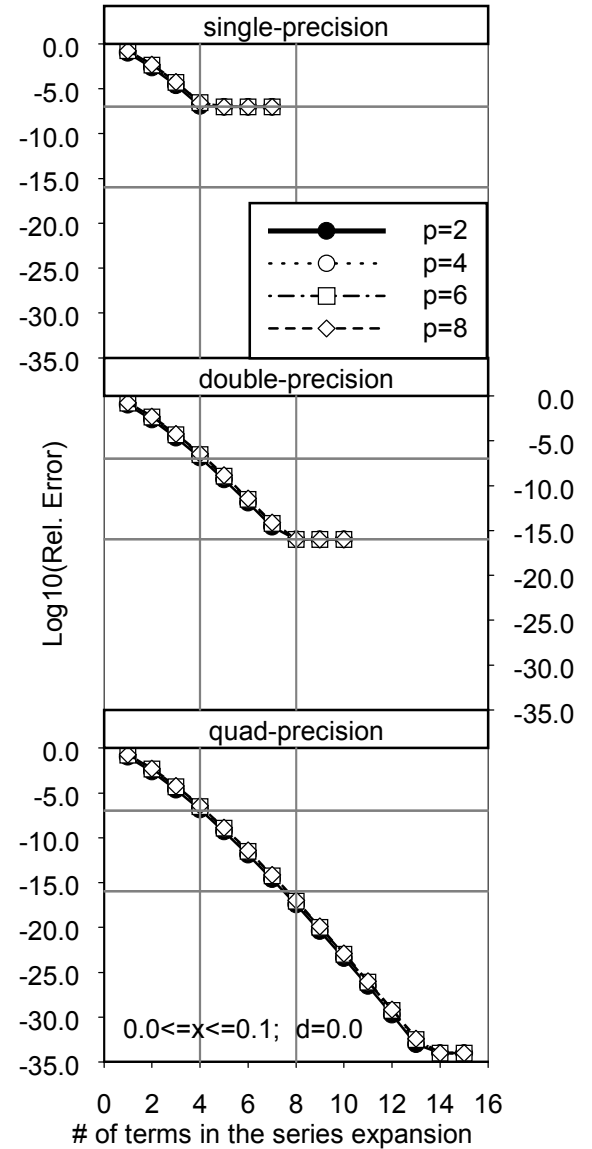
Fig5. Convergence curves for integrals with even values of p.

Consider $I_p = \int\limits_{u_1}^{u_2} \dfrac{u^p e^{-jkR}}{R} du$ where $R = \sqrt{u^2 + \delta^2}$. With the substitution $dR = \dfrac{udu}{R}$

we get $I_p = \int u^{p-1} e^{-jkR} dR$. When p is odd, this integral can be solved analytically.
For example:

$$p = 1;\ I_p = \left. \frac{je^{-jkR}}{k} \right|_{u_1}^{u_2} \tag{17a}$$

$$p = 3;\ I_p = \left[e^{-jkR} \left[u^2 \left(\frac{j}{k}\right) - 2R \left(\frac{j}{k}\right)^2 + 2\left(\frac{j}{k}\right)^3 \right] \right]_{u_1}^{u_2} \tag{17b}$$

$$p = 5;\ I_p = \left[\frac{je^{-jkR}}{k} \left[u^4 - 4\left[u^2 R + (\delta^2 - 3R^2) \right] \left(\frac{j}{k}\right) + 6R\left(\frac{j}{k}\right)^2 - 6\left(\frac{j}{k}\right)^3 \right] \right]_{u_1}^{u_2} \tag{17c}$$

Equation Set III. Examples of analytical solutions for the integral for odd p.

Application to the Magnetic Vector Potential.

The application of the above procedure to double integrals is straightforward. The inner integral is computed as above and then a quadrature integration formula is applied to the outer integral.

Cartesian coordinates. A double integral of interest is given by:

$$I_{Cart} = \int\limits_{y}^{y_2} dy \int\limits_{x_1}^{x_2} (x - x_0)^p \frac{e^{-jkR}}{R} dx \qquad \text{where}$$

$$R = \sqrt{(x - x_0)^2 + (y - y_0)^2 + z_0^2}.$$

The surface is in the x-y plane and the test point is at (x_0, y_0, z_0). In terms of the inner integral we replace $(x - x_0)$ by u, $((y - y_0)^2 + z_0^2)$ by δ^2 and adjust the integration limits appropriately.

Cylindrical coordinates. Here, the double integral is given by:

$$I_{cyl} = \frac{1}{2\pi} \int\limits_{0}^{2\pi} d\phi \int\limits_{z_1}^{z_2} (z - z_0)^p \frac{e^{-jkR}}{R} dz \text{ where } R =$$

$$\sqrt{(z - z_0)^2 + (\Delta\rho_0)^2 + 4a(a + \Delta\rho_0)\sin^2\phi}$$

The surface is that of a cylinder of radius a, and with $\Delta\rho_0 \geq -a$ the test point is at $(a + \Delta\rho_0, 0, z_0)$. In this instance $\delta^2 = (\Delta\rho_0)^2 + 4a(a + \Delta\rho_0)\sin^2\phi$ and $u = (z - z_0)$ and again the limits of integration are appropriately adjusted.

The results for the calculation of the MVP for a section of a cylindrical dipole with values of $a = 0.007\lambda$ and $0.0 \leq z \leq 0.1$ are shown in Figures 6a and 6b. Two quadrature methods were investigated – the Gauss-Legendre method and the Linlog method [12]. The reason for choosing the latter method is that the series containing even p always contains log terms in its real component. Linlog was designed specifically to integrate functions that contain polynomials and logarithmic terms.

Both sets of calculations were performed in quad precision. The reference values were calculated using 42 terms with the respective quadrature methods. The superiority of the Linlog approach, when applied for even powers of p, is clearly visible. The relative error is seen to reach a level of approximately –21.4 and then remains constant. The nodes and weights, as originally reported, are only known to 20 digits, hence the observation is hardly surprising. This, then, is the bound on
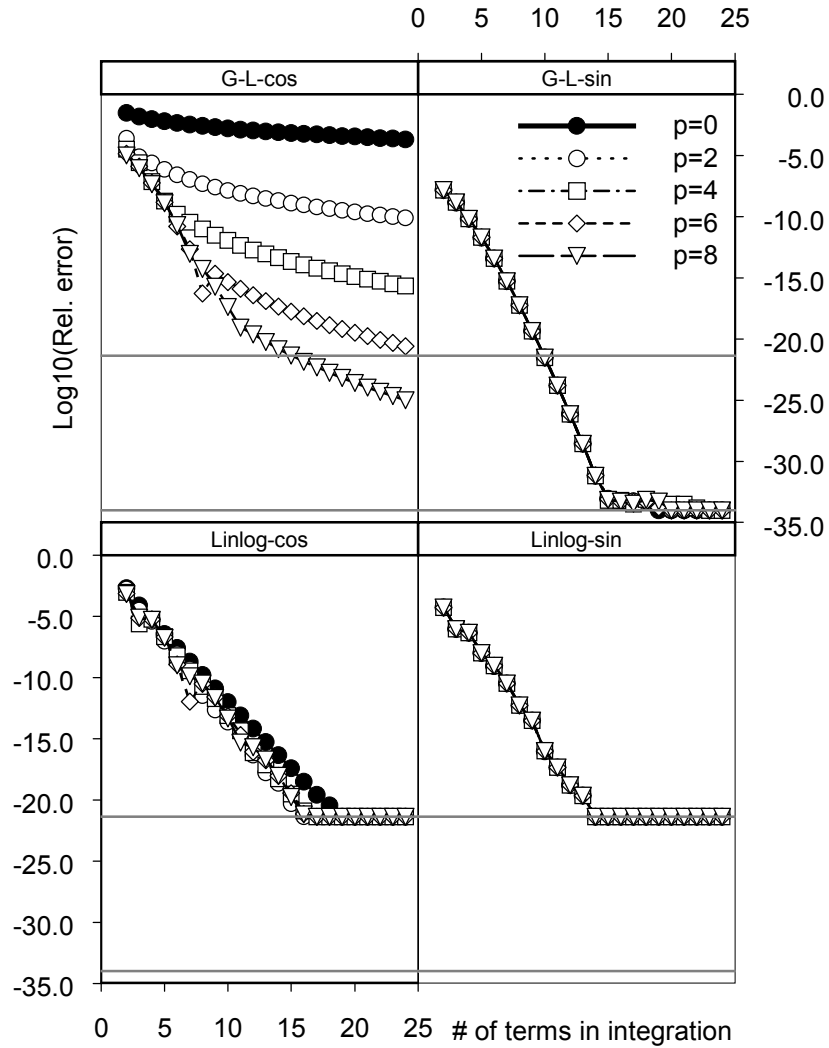
Figure 6a. Performance of two integration methods on the real and imaginary parts of the magnetic vector potential on the surface of a cylindrical dipole, for even values of p.
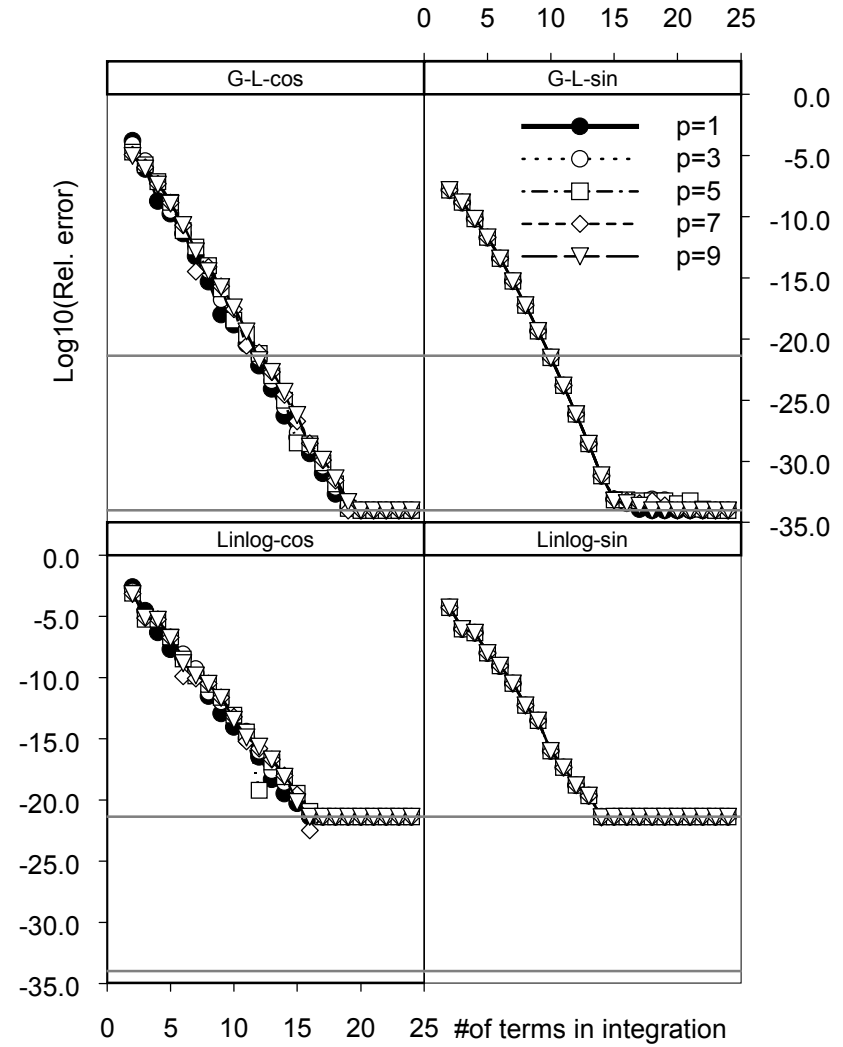
Figure 6b. Performance of two integration methods on the real and imaginary parts of the magnetic vector potential on the surface of a cylindrical dipole, for odd values of p.

the accuracy to which this particular MVP can be calculated using today's tools.

It remains to examine the effect of the offset value as was done for the Duffy transform and reported in Table III. Again the work is done in double precision and is for $p = 0$. The ensuing results are shown in Table IV. Compared with the results in Table III, it is clear that the value of the offset has little effect on the number of terms needed to achieve a relative accuracy equal to the machine precision.

Offset	Outer	Series	Total
0.0	14	8	112
0.1	17	9	153
0.01	23	7	161
0.001	24	8	192
0.0001	24	7	168

Table IV. The effect of the offset values on the number of integration terms for the cylindrical surface using the term-by-term integration of a Maclaurin series.

Comparison Between Duffy and SEIS.

The efficiency of the calculation of the MVP by the two methods – the Duffy transform and the SEIS method – was investigated for the cylindrical case already discussed. In the case of the Duffy transform the number of function evaluations of both inner integrals was counted. In the case of the SEIS the count was the product of the number of nodes in the outer integral and the number of terms in the series expansion. The results are shown in Figure 7. The reference line is located at πa. It appears that both methods are most efficient when the aspect ratio of the cell under consideration is approximately 1:1. The Duffy transform is particularly susceptible to this phenomenon. In the case of the SEIS approach, at the high end of the z range, the number increases as the value of z increases – due to the need for more terms in the series expansion. At the low end of the range, the number of terms needed in the series expansion falls off – but the number of nodes needed in the Linlog integration increases.
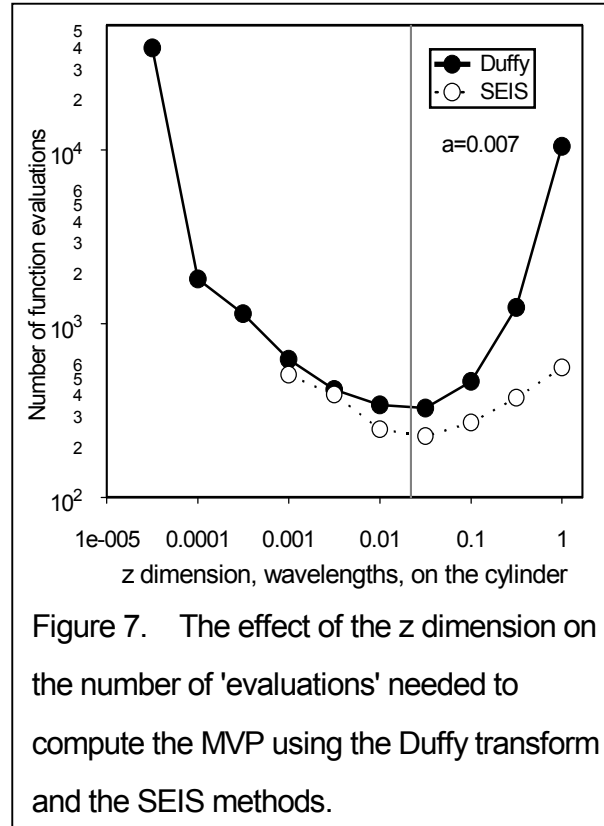
Figure 7.   The effect of the z dimension on the number of 'evaluations' needed to compute the MVP using the Duffy transform and the SEIS methods.

In this example, the number of integration nodes needed for z=0.001 was 39.

Key Findings

1)   It was shown that conventional numerical methods give misleading results when integrating the Green's function. Consider the results of Figure 2a.   When $\delta = 0.0001$ the relative error changes very little as the number of integration terms is increased until very large numbers of terms are employed.   The slow improvement in the error curve would normally be interpreted as convergence – leading to an inaccurate evaluation. It was shown that this behavior is a direct consequence of the derivatives in the neighborhood of $u = 0$.

2)   The results presented in Figures 2a and 6 emphatically illustrate the poor performance of Gauss-Legendre methods for evaluating the real component of any of the integrals studied. This finding is applicable to all quadrature methods that are applied directly to this class of problem.

3)   The Duffy transform provides a reliable method for computing the MVP when the test point is on the surface.   As implemented here, it is not suitable for use when the test point is off the surface.   It has the advantage that the integrals can be evaluated using standard integration techniques such as Gauss-Legendre.

4)   The use of a Maclaurin expansion of the Green's function, followed by term by term integration and careful summation provides a stable means for calculating both the real and imaginary components of the function.   The method is efficient and can be used both on and off the surface being examined.

5)   Analytical solutions for the integral of the Green's function and its product with polynomial representations, of odd degree, of the surface current have been presented. These solutions provide a method for evaluating both the convergence and the accuracy of the series-expansion-integration-summation approach.

6)   The analytical results presented for current representations of odd degree would appear to offer an accurate and efficient approach to the evaluation of those integrals. However, it was found that rounding errors seriously degraded the accuracy of such calculations when the range of integration was small and such an approach should be avoided unless high precision software is employed.

7)   The algorithm used for the outer integral, when using the series expansion-integration-summation approach must recognize the presence of the logarithmic terms in the series expansion when p is even.   This means using the Linlog method [12] for this particular integration.

Final Remarks

The calculation of integrals associated with the magnetic vector potential has been examined in depth.   The integration of the Green's function should not be attempted with quadrature methods, unless some suitable transformation to remove the singularity has been undertaken.   An example of the latter is the transform due to Duffy, and this is quite suitable when the test point is on the surface. For all-round performance, it is proposed that the inner integral, that includes the Green's function, be evaluated by means of the integration of each term of a Maclaurin expansion.   The outer integral can then be evaluated using the Linlog rule.   In all cases, the integration can be taken to the precision of the machine/compiler (single, double or extended/quad), except that the Linlog nodes/weights currently limit the relative error to approximately 20 digits.   The integration of the Maclaurin series prior to summation provides a method that is efficient and accurate.

References.

[1]   A. F. Peterson, S. L. Ray, R. Mittra, *Computational Methods for Electromagnetics*, IEEE Press, 1998.
[2]   D. B. Miron, "The Singular Integral Problem in Surfaces", *IEEE Trans. Ant. & Prop.*, Vol. AP-31, No. 3, pp. 507-509, May 1983.
[3]   A. D. Yaghijan, "Electric Dyadic Green's Functions in the Source Region", *Proc. IEEE*, Vol. 68, No. 2, pp. 248-263, Feb. 1980.
[4]   E. K. Miller, "A Computational Study of the Effect of Matrix Size and Type, Condition Number, Coefficient Accuracy and Computation Precision on Matrix-Solution Accuracy", *Intl. Symp. On Ant. & Prop. Digest, Newport Beach, CA*, pp. 1020-1023, June 1995.
[5]   M. G. Duffy, "Quadrature Over a Pyramid or Cube of Integrands with a Singularity at a Vertex", *SIAM J. Numer. Anal.*, Vol. 19, No. 6, pp. 1260-1262, Dec. 1982.
[6]   M. L. Overton, *Numerical Computing with IEEE Floating Point Arithmetic*, SIAM, 2001.
[7]   D. R. Wilton, C. M. Butler, "Effective Methods for Solving Integral and Integro-

Differential Equations", *Electromagnetics*, Vol. 1, pp. 289-308, 1981.

[8] J. M. Song, W. C. Chew, "Moment Method Solutions Using Parametric Geometry", *J. of Electromagnetic Waves and Appl.*, Vol. 9, pp. 71-83, 1995.

[9] A. Herschlein, J. v. Hagen, W. Wiesbeck, "Methods for the Evaluation of Regular, Weakly Singular and Strongly Singular Surface Reaction Integrals Arising in Method of Moments", *ACES Journal,* Vol. 15, No. 1, pp. 63-73, March 2002.

[10] M. Gimersky, S. Amari, J. Bornemann, "Numerical Evaluation of the Two-Dimensional Generalized Exponential Integral", *IEEE Trans. Ant. & Prop.,* Vol. AP-44, No. 10, pp. 1422-1425, 1996.

[11] D. H. Bailey, "A Portable High Performance Multi-precision Package", *RNR Technical Report RNR-90-022*, May 18, 1993. See also www.nersc.gov/~dhbailey/mpdist/.

[12] J. H. Ma, V. Rohklin, S. Wandzura, "Generalized Gaussian Quadrature Rules for Systems of Arbitrary Functions", *SIAM J. Numer. Anal.,* Vol. 33, pp. 971-996, June 1996.

Addendum: Procedural Considerations.

In order to assure the best possible accuracy when evaluating series such as those in equations (12) - (15), several "good practice" issues need to be followed.

1) Terms that are to be added need to be stored separately from those that are to be subtracted. Thus the values associated with the upper limit in an integration formula must be separated from those associated with the lower limit of integration. A similar separation should be maintained when implementing the Maclaurin series, noting that this involves the additional complication of a series with alternating signs.

2) When evaluating the terms associated with the real part of the overall integral, negative values may occur due to the presence of the log term. These should be identified and stored appropriately.

3) Terms should be added by starting with the smallest and proceeding to the largest. To this end, the two sets of terms need to be sorted in ascending order prior to summation.

4) There is considerable repetition in the components from one term to the next. This observation can be exploited to create a fast, resource-conserving algorithm.

Malcolm M. Bibby received the B.Eng. and Ph.D. degrees in Electrical Engineering from the University of Liverpool, England in 1962 and 1965 respectively. He has been interested in the numerical aspects associated with antenna design for the last twenty years.

Andrew F. Peterson received the B.S., M.S., and Ph.D. degrees in Electrical Engineering from the University of Illinois, Urbana-Champaign in 1982, 1983, and 1986 respectively. Since 1989, he has been a member of the faculty of the School of Electrical and Computer Engineering at the Georgia Institute of Technology, where he is now Professor and Associate Chair for Faculty Development. Within ACES, he served for six years (1991-1997) as a member of the Board of Directors, and has been the Finance Committee Chair and the Publications Committee Chair.